

Journal of
Applied Remote Sensing

RemoteSensing.SPIEDigitalLibrary.org

Global analysis and forecast impact assessment of CubeSat MicroMAS-2 on numerical weather prediction

Narges Shahroudi
Yan Zhou
Sid-Ahmed Boukabara
Kayo Ide
Tong Zhu
Ross Hoffman

SPIE.

Narges Shahroudi, Yan Zhou, Sid-Ahmed Boukabara, Kayo Ide, Tong Zhu, Ross Hoffman, "Global analysis and forecast impact assessment of CubeSat MicroMAS-2 on numerical weather prediction," *J. Appl. Remote Sens.* **13**(3), 032511 (2019), doi: 10.1117/1.JRS.13.032511.

Global analysis and forecast impact assessment of CubeSat MicroMAS-2 on numerical weather prediction

Narges Shahroudi,^{a,b,*} Yan Zhou,^{a,c} Sid-Ahmed Boukabara,^a Kayo Ide,^d
Tong Zhu,^{a,e} and Ross Hoffman^{a,c}

^aNOAA/NESDIS/Center for Satellite Applications and Research, College Park, Maryland, United States

^bRiverside Technology Inc., College Park, Maryland, United States

^cUniversity of Maryland, Earth System Science Interdisciplinary Center, College Park, Maryland, United States

^dUniversity of Maryland, College Park, Maryland, United States

^eColorado State University, Cooperative Institute for Research in the Atmosphere, Fort Collins, Colorado, United States

Abstract. The Micro-Sized Microwave Atmospheric Satellite (MicroMAS-2) is a 12-channel passive microwave radiometer on a CubeSat developed by Massachusetts Institute of Technology Lincoln Laboratory. MicroMAS-2 observations (1) enhance the current observing system capabilities and (2) mitigate the potential loss of some existing observations. Observing System Simulation Experiments (OSSEs) quantitatively estimate the expected impact of adding the MicroMAS-2 to the current global operational analysis and forecast systems or to a data gap scenario. First, MicroMAS-2 data on one low Earth-orbiting platform were simulated by the Community Radiative Transfer Model from the NASA GEOS-5 Nature Run, which serves as the truth in the OSSE. The assimilation of the MicroMAS-2 observations into the research version of the January 2015 NOAA Global Data Assimilation System in addition to the current operational observation system and in addition to a data gap scenario shows improvement on both analysis and forecast performance skills. © 2019 Society of Photo-Optical Instrumentation Engineers (SPIE) [DOI: [10.1117/1.JRS.13.032511](https://doi.org/10.1117/1.JRS.13.032511)]

Keywords: data assimilation; observing system simulation experiments; CubeSat; numerical weather prediction; microwave sounder.

Paper 190231SS received Mar. 29, 2019; accepted for publication Jul. 24, 2019; published online Aug. 13, 2019.

1 Introduction

Current Earth-observing satellite-based microwave (MW) radiometers that are designed to collect atmospheric profile data such as the Advanced Technology Microwave Sounder (ATMS) and the Special Sensor Microwave Imager/Sounder (SSMIS) are very costly and require a long time to develop and launch. Cube Satellites (CubeSats) seek to implement data collection capabilities on a much smaller scale that can be accomplished with lower costs and shorter development times. CubeSats are SmallSats built from one or more 10 cm cubes or units. A CubeSat made of n 10 cm cubes is called an n -unit or nU CubeSat. The Micro-Sized Microwave Atmospheric Satellite (MicroMAS-2) mission is a small, low-cost 3U CubeSat containing a miniaturized microwave scanner. MicroMAS-2 observes atmospheric temperature with seven channels near the 118.75-GHz oxygen absorption line, water vapor with three channels near the 183-GHz water vapor absorption line, precipitation with a single channel near 90 GHz, and cloud ice with a single channel at 205 GHz.¹

The goal of this study is to assess the potential benefit of a MicroMAS-2 instrument on global Numerical Weather Prediction (NWP) applications by conducting Observing System Simulation Experiments (OSSEs^{2,3}). A MicroMAS-2 impact study using a regional OSSE on a local severe

*Address all correspondence to Narges Shahroudi, E-mail: narges.shahroudi@noaa.gov

storm was carried by Li et al.⁴ The basic principle of an OSSE is to assimilate synthetic observations derived from an atmospheric model run, known as the nature run (NR) and assumed to represent the truth, and then to determine the impact of the simulated observations on weather forecast models. The Community Global OSSE Package (CGOP) has been developed at the Center for Satellite Applications and Research (STAR) at NOAA to conduct OSSEs.⁵⁻⁷ The CGOP is an evolving package. Currently in the CGOP, the truth is taken to be the GEOS-5 nature run (G5NR), a 2-year (May 2005 to May 2007), 7-km-resolution, nonhydrostatic simulation created with the Goddard Earth Observing System Model, version 5 (GEOS-5) developed by NASA.⁸ Then, geophysical profiles of temperature and moisture evaluated from the G5NR are input to forward operators to simulate error-free observations. These forward operators include the Community Radiative Transfer Model (CRTM^{9,10}) and the Global Positioning System Radio Occultation (GPS-RO) observation simulator developed by NOAA.¹¹ Observation error is added following a procedure developed by NASA.¹² The simulated observations are assimilated by a hybrid 3D-ensemble variational (3D-EnVar) or 4D-ensemble variational (4D-EnVar) data assimilation (DA) system made available by NOAA.^{13,14} This study employs the research version of the January 2015 NOAA Global Data Assimilation System (GDAS).

Four experiments are conducted in order to consider MicroMAS-2 as an addition to ATMS or as a replacement for ATMS in the Suomi National Polar-orbiting Partnership (SNPP) orbit. For the first comparison, experiment control assimilates the current operational suite of observations. Experiment Control + MicroMAS-2 adds MicroMAS-2 observations to control. The key question here is whether the MicroMAS-2 channel set adds value to the existing ATMS on SNPP. For the second comparison, the baseline experiment 2Polar is a stringent data gap scenario experiment, in which there are no afternoon polar orbiting meteorological satellites. Experiment 2Polar + MicroMAS-2 adds the same MicroMAS-2 observations to the 2Polar observations as were added to Control + MicroMAS-2. Here, the key question is to assess the value of MicroMAS-2 in this very limited data scenario. In the present experiments, no explicit errors are added to the simulated observations, but differences between the G5NR and the Global Forecast System (GFS) model used in the DA and forecast experiment result in some representativeness error.

This paper is organized as follows: Sec. 2 includes a summary description of the MicroMAS-2 instrument, the characteristics of the MicroMAS-2 brightness temperature (BT) observations, the sensor simulation methodology for MicroMAS-2 BTs, and a geophysical capability assessment, which includes the validation of the data quality in terms of both BT and retrieved geophysical variables. Section 3 describes the experiments and verification methodology. The impact assessment of assimilating MicroMAS-2 on the NWP analysis and forecast quality is presented in Sec. 4, and a concluding summary is given in Sec. 5. All observations used in the OSSEs are simulated for cloud-free conditions and without explicit observation errors. These limitations are mitigated by the quality control (QC) procedures used in the DA system (see Sec. 2.4) and the findings of Boukabara et al.⁷ that relative impacts for such “perfect” observation OSSEs closely match those for real data observing system experiments (OSEs) (see Sec. 5).

2 MicroMAS-2

2.1 Sensor Description

MicroMAS-2 developed at the Massachusetts Institute of Technology (MIT) Lincoln Laboratory is a dual-spinning 3U CubeSat equipped with a passive microwave spectrometer with 12 channels including channels for temperature and water vapor soundings. The first satellite in the series, MicroMAS-2a, was launched January 12, 2018, into a sun synchronous orbit at an altitude of 550 km. The second, MicroMAS-2b is scheduled to be launched imminently. Table 1 lists the MicroMAS-2 channel central frequencies.

MicroMAS-2 exploits several frequencies around the 118-GHz oxygen band which allow the use of smaller antennas and are thus favored for small satellites. Channels 2 to 8 have no equivalent existing space-borne sensor channel but are very similar to the 60-GHz channels on ATMS and the Advanced Microwave Sounding Unit-A (AMSUA). Figure 1(a) shows the weighting

Table 1 MicroMas-2 channels frequencies with their corresponding channels from heritage instruments. The EOE standard deviation is used in the DA system.

MicroMas-2 channel	Frequency (GHz)	Matching sensor	EOE (K)	Sensitivity
1	91.65	SSMIS-91.65	1.50	Precipitation
2	114.85	AMSUA-50.30/52.80	3.00	Temperature
3	115.47	AMSUA-50.30/52.80	3.00	Temperature
4	116.10	AMSUA-53.590.1/52.80	0.55	Temperature
5	116.72	AMSUA-52.80	0.55	Temperature
6	117.34	AMSUA-53.590.1	0.40	Temperature
7	117.97	AMSUA-54.94/55.50	0.40	Temperature
8	118.59	AMSUA-57.29/57.290.2	0.40	Temperature
9	183.31	AMSUB-183.311	2.50	Water Vapor
10	183.313	AMSUB-183.313	2.50	Water Vapor
11	183.317	AMSUB-183.317	2.50	Water Vapor
12	205.3	ATMS-165.5	2.50	Cloud Ice

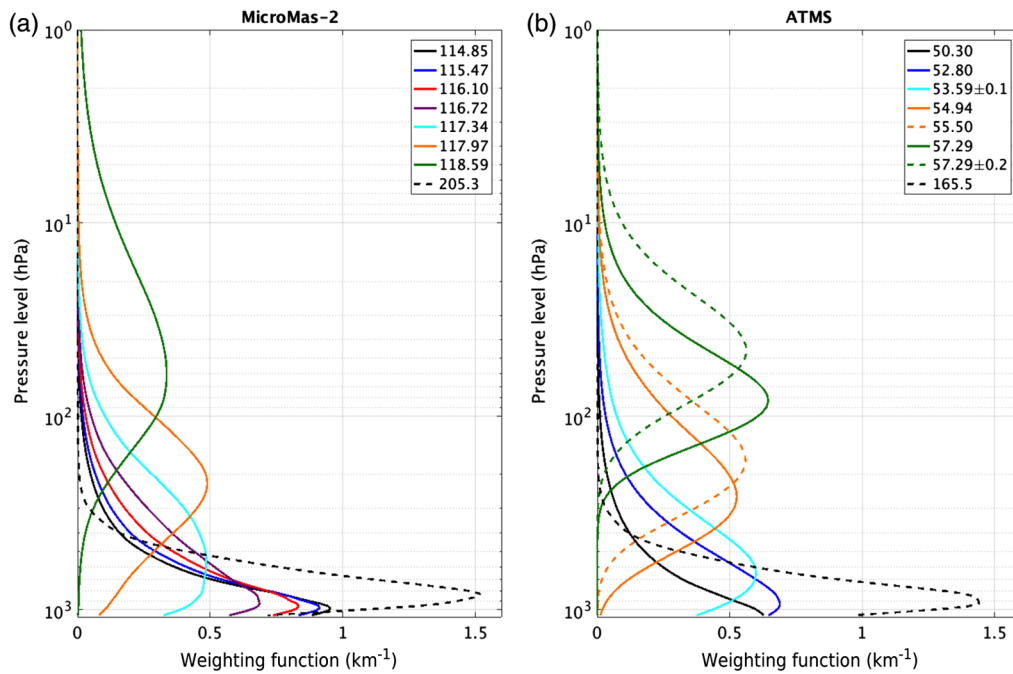


Fig. 1 The (a) MicroMas-2 and (b) ATMS weighting function (km^{-1}) for a standard atmosphere as functions of pressure (hPa).

functions in a standard atmosphere for the channels of MicroMAS-2. For comparison, Fig. 1(b) shows the weighting functions for the corresponding channels on the SNPP ATMS sensor. MicroMAS-2 channels at 114.85, 115.47, 116.10, and 116.72 GHz (black, blue, red, and magenta) are maximum at the same pressure level as ATMS channels 50.30 and 52.80 GHz (black and blue), but the peaks for the MicroMAS-2 weighting functions are much closer together. MicroMAS-2 channel 117.34 GHz is similar to ATMS channel 53.59 ± 0.1 (both aqua). MicroMAS-2 channel 117.97 GHz (orange) is intermediate to ATMS channels 54.94 and 55.50 GHz (orange, solid, and dashed) and MicroMAS-2 channel 118.59 GHz is intermediate to

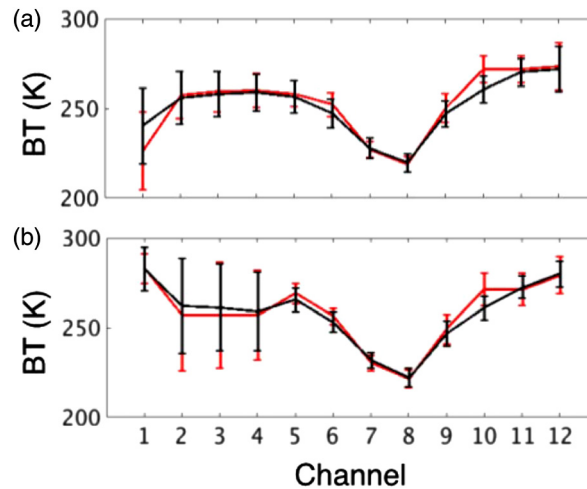


Fig. 2 Mean (lines) and standard deviation (± 1 standard deviation error bars) of the perfect simulated observations (black) and real (channels 1, 9 to 11) or predicted (channels 2 to 8, 12) observations (red) versus MicroMAS-2 channel number for (a) ocean and (b) land.

ATMS channels 57.29 and 57.29 ± 0.2 GHz (all green). Finally, MicroMAS-2 channel 205 GHz is similar to ATMS channel 165.5 GHz (both black dashed).

2.2 Simulation

The process to create the perfect (i.e., with no explicit error added) simulated satellite observations is to interpolate the atmospheric profiles of temperature, water vapor, and atmospheric gases from G5NR data linearly in latitude and longitude and time to the location of existing real satellite observations. These profiles along with surface properties and observing geometry of the sensor are the inputs to the forward operator, CRTM. CRTM is used to simulate all satellite radiometer channels used in this study, including MicroMAS-2 and all other MW and infrared (IR) profilers. CRTM requires no vertical interpolation: here, for simulation, CRTM uses the G5NR vertical structure. For DA, in the Gridpoint Statistical Interpolation analysis system (GSI), CRTM uses the GFS vertical structure. For the calculation of optical depth, CRTM uses “coefficients” tables for each sensor. The sensor coefficients are determined by best fitting the fast optical depth model to values calculated by the very accurate and computationally expensive Line-by-Line Radiative Transfer Model.¹⁵ Therefore, the calculated optical depths are valid for the range of profiles (of temperature, water vapor, and other gases) in the training datasets used. CRTM outputs are the channel radiances and/or BTs. All the radiance simulations are made clear sky by setting the cloud liquid and ice water to zero. However, BT observations that would be affected by clouds are not assimilated in our experiments. (See discussion in Sec. 2.4 related to Fig. 4.)

To simulate MicroMAS-2, the timing and locations of the observations and its observing geometry must be defined. As noted in Sec. 1, MicroMAS-2 is being considered in this study as a replacement for or addition to ATMS. Therefore, for the purpose of this study, the observation latitude, longitude, time, scan angle, and zenith angle from ATMS on SNPP were extracted and used as the template for the MicroMAS-2 simulations. The MicroMAS-2 “coefficients” were determined based on the sensors characteristics provided by MIT Lincoln Lab.¹⁶ The simulated MicroMAS-2 BT observations for all 12 channels were created for the period of 1 August 1 to September 15, 2006.

2.3 Validation

As described in Sec. 2.1, some channels of the MicroMAS-2 have no equivalent existing spaceborne sensor channel. To benchmark these new proposed channels such as at 118 GHz, Boukabara et al.⁶ used a multiple linear regression of simulated data to relate these new observations to existing channels from ATMS for which real data are available and which have similar

sensitivities to atmospheric conditions. The validation then compares observations simulated from the NR to observations predicted by the regression relationship applied to actual real observations of the existing channels. A detailed description of the methodology and validation is described in Ref. 6. Validation included both initial day comparisons (not shown) and statistical comparisons. Initial day comparisons are possible for the G5NR initial day by comparing AMSU-B to simulated MicroMAS-2 183 GHz water vapor channels (Ref. 6; Fig. 9). However, with no ATMS data available for 2006, only statistical comparisons are possible for some channels. This comparison for a one-month period between simulated MicroMAS-2 (G5NR August 2006) and the real observations of ATMS and SSMIS (August 2014) show reasonably good statistical agreement. Figure 2 is an extract from this latter analysis of Ref. 6; Fig. 9. Statistics in Fig. 2 show (1) there is good agreement for the temperature sounding channel BTs (channels 2 to 8), (2) the simulated water vapor channel BTs (channels 9 to 11) are cooler than observed, and (3) the precipitation channel (channel 1) BTs agree well over land but over ocean the simulated BTs are much cooler.

2.4 Preassimilation Data Quality Assessment

The focus of this study is to assess the impact of assimilating perfect simulated MicroMAS-2 observations into the GDAS/GFS. Typical coverage for a single 6-h DA window is shown in Fig. 3. Figure 3 shows the observations for channel 1 we actually use in the OSSEs described in detail below in Sec. 3.1. The preassimilation data quality assessment consists of comparisons of simulated observations with real AMSU, ATMS, and SSMIS observations to characterize biases, errors, and the effectiveness of QC algorithms. The results of the assessment help to specify how the data are assimilated, including what observation errors (weights) to assign MicroMAS-2 channels and how to implement QC procedures. The estimated observation errors (EOEs) to be used in the analysis for each MicroMAS-2 channel were taken from a similar channel of an existing sensor.

The EOE includes representativeness errors due to the differences in scales between the observations and the analysis as well as forward errors problem (e.g., the simulation of BTs). It is generally a good approximation to assume that the EOE for MW BTs are the same for similar channels on similar instruments. However, the reciprocal of EOE squared may be considered the observations weight, which should be tuned in future experiments. The corresponding channels and the observation error for each MicroMAS-2 channel are given in Table 1. Note that because the errors given in Table 1 are for use in the DA system and include representativeness and forward model errors, MicroMAS-2 channels sensitive to the surface have higher observations error than the temperature sounding channels, as is the case for other MW sensors. Note however, that in Fig. 1(a), MicroMAS-2 channels 2, 3, 4, and 5 are all peaking near the surface, and are all equally likely to be affected by the surface. Since there is not much difference between the pressures of these peaks, the weighting functions make it appear that these four channels do not have much independent information. However, following the EOE given for

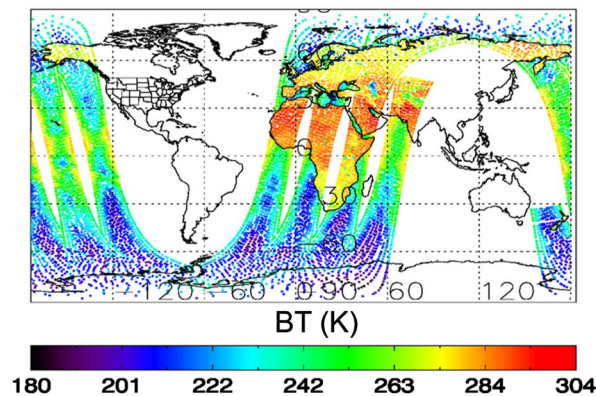


Fig. 3 Simulated BT (K) for MicroMAS-2 Channel 1 (91.65 GHz) on SNPP orbit for 0000 UTC August 8, 2006.

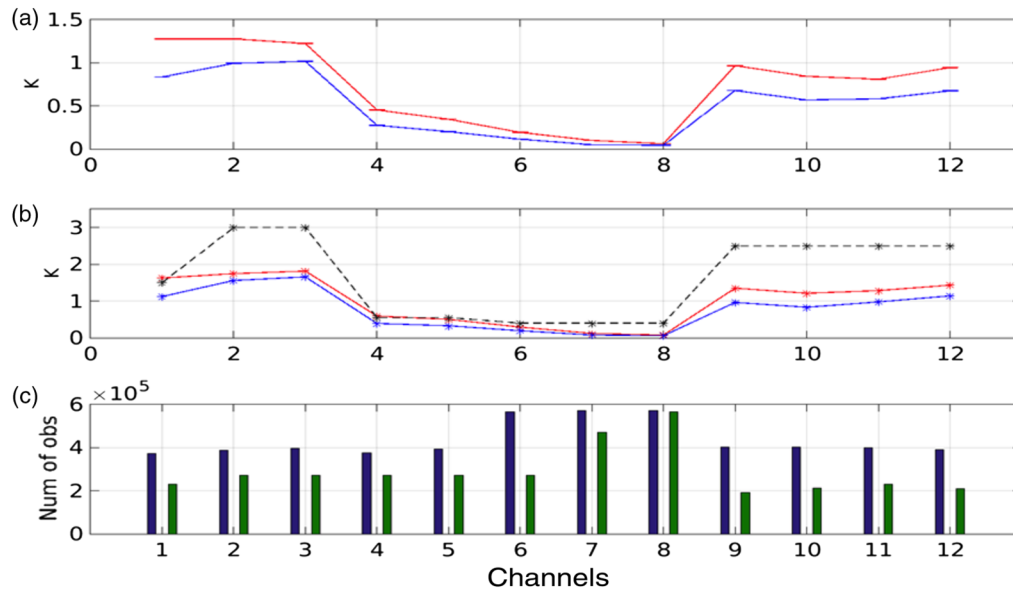


Fig. 4 MicroMAS-2 BT DA diagnostics for each channel averaged over the first 2 weeks of the Control + MicroMAS-2 experiment (August 15 to 28, 2006) for (a) global mean of O-A and O-B (blue and red, K), (b) global standard deviation of O-A and O-B (blue and red, K), and (c) the number of observations assimilated (counts/day) for simulated MicroMAS-2 (blue) compared to real ATMS (red) from a Control OSE. The EOE standard deviations from Table 1 are plotted as a black dashed line in (b).

AMSU-A in GSI, we assign channels 2 and 3 with high EOE and channels 4 and 5 with low EOE (Table 1).

The QC routine that was implemented for MicroMAS-2 in the DA system is analogous to that for AMSU and ATMS. First, the QC rejects any BT observations where the cloud liquid water (CLW) amount in the background is greater than 0.5 kg m^{-2} . Thus although clear-sky radiances are simulated everywhere, they are not assimilated where there are clouds. In fact, because G5NR has CLW amounts generally higher than reality, we expect that there will be fewer MW observations used in the OSSE than in reality. Then, BTs adversely affected by surface emissivity are eliminated. Finally, a background check removes any points where the departure of the MicroMAS-2 observation from the background (O-B) exceeds three times the observation error.

Figures 4(a) and 4(b) show the O-A and O-B statistics after assimilating MicroMAS-2 observations and applying the QC and bias correction. Both bias and standard deviation of O-A and O-B are larger for channels (1 to 3 and 9 to 12) that are affected by the surface and water vapor. For the upper tropospheric temperature channels (4 to 8), bias and standard deviation values are all small compared to 1 K, and the reductions in these error measures due to the analysis are on the order of 0.1 K. The other channels have biases of ~ 1 K and standard deviations of 1 to 2 K. As a percentage of the O-B value, these reductions range from 10% to 40%.

The results of applying the QC procedures to the MicroMAS-2 BT observations showed that approximately the same numbers of observations are assimilated for each channel of MicroMAS-2 as for the corresponding existing channel [Fig. 4(c)]. Note that agreement between the number of MicroMAS-2 observations used in the OSSE and the number of ATMS observations used in the real data OSE justifies the use of clear sky BTs along with the QC test based on the background CLW.

3 Description of the Experiments and Verification Methodology

3.1 Experiment Setup

For assessing the impact of MicroMAS-2 on analysis and forecast skills on GDAS/GFS, the simulated observations were assimilated into the GSI. The GSI ingests and assimilates satellite

radiances, atmospheric motion vectors (AMVs), GPS-RO observations, and conventional observations such as radiosondes and aircraft. For an OSSE, all these observations are available in perfect simulated format.^{5,6} The MicroMAS-2 observations were simulated and validated and have been prepared for assimilation as described in Sec. 2. Four OSSEs were configured and run to assess the impact of adding MicroMAS-2 on the analysis and forecast skills:

- Control: All observations used in 2014 operational implementation of GDAS/GFS (see Table 2)
- 2Polar: This experiment reduces satellite observation coverage from polar orbiting satellites to a 2-Polar configuration in which all secondary and backup polar satellites and all satellites in afternoon orbits are eliminated. The only remaining polar orbiting satellite observations are from F18 and MetOp-B. Other satellite observations are retained including BTs from GEO platforms, AMVs, and GPS-RO refractivities.
- Control + MicroMAS-2: Adds one MicroMAS-2 on SNPP orbit to Control.
- 2Polar + MicroMAS-2: Adds one MicroMAS-2 on SNPP orbit to 2Polar.

Experiment Control began on 1800 UTC July 31st, 2006. The other three experiments started with Control's 1800 UTC August 7th analysis. A 7-day spin up covering August 8th to August 15th was included in each experiment, and the period from 0000 UTC August 15th to September 15th was used for assessment.

Table 2 Satellite data assimilated in Control.

Platform	Sensor(s)	Type; orbit
Aqua	AIRS, AMSUA	MW, IR; early morning
F17	SSMIS	MW; early morning
F18	SSMIS	MW; early morning
GOES-15	SNDR	IR; GEO
Meteosat-10	SEVIRI	IR; GEO
MetOp-A	AMSUA, MHS, IASI, HIRS4	MW, IR; mid-morning
MetOp-B	AMSUA, MHS, IASI	MW, IR; mid-morning
NOAA-15	AMSUA	MW; afternoon
NOAA-18	AMSUA, MHS	MW; afternoon
NOAA-19	AMSUA, MHS	MW; afternoon
SNPP	ATMS, CrIS	MW, IR; afternoon
Coriolis	WindSat	MW; early morning
GOES -15	AMV	IR; GEO
JMA	AMV	IR; GEO
Meteosat	AMV	IR; GEO
COSMIC	GPS-RO	RO; LEO
MetOp-A	GRAS	RO; mid-morning
MetOp-B	GRAS	RO; mid-morning
TerraSAR-X	GPS-RO	RO; dawn-dusk
GRACE	GPS-RO	RO; LEO
Conventional	<i>In situ</i>	—

The OSSEs were run using the 2015 operational hybrid 3DEnVar version of GDAS at the research resolutions. The analysis, including the ensemble, cycles every 6 h at 0000, 0600, 1200, and 1800 UTC and uses T254 (about 50 km) horizontal resolution and 64 vertical levels. The deterministic 168 h forecast starts at 0000 UTC each day using T670 (about 25 km) horizontal resolution and the same 64 vertical levels.

3.2 Verification Methodology

A variety of assessment metrics can be used to assess the impact of MicroMAS-2 on the GDAS analyses and GFS forecasts. The primary assessment metrics (PAMs) that will be used in this study are for various (1) forecast times [0, 24, 48, 72, 96, 120, 144, 168 h]; (2) pressure levels [10 to 1000 hPa]; (3) domains [global, North America, Northern Hemisphere extratropics (NHX), Southern Hemisphere extratropics (SHX), tropics]; (4) variables [geopotential height (Z), temperature (T), vector wind (V), relative humidity (RH)]; (5) statistics [bias or absolute mean error (AME), standard deviation, anomaly correlation (AC) root-mean square error (RMSE)]; (6) verification time [0000 UTC for the 32 days from August 15, to September 15]; and (7) experiment [Control, Control + MicroMAS-2, 2Polar, and 2Polar + MicroMAS-2].

To assess the impact on the GDAS analysis, the bias and error standard deviation of the analysis were calculated for Z , T , and RH for different levels in terms of maps, profiles, and tables. To assess the impact on the GFS forecast, the RMSE and AC were calculated for Z , T , RH, and V for different forecast time, different levels, and different domains in terms of statistics, maps, and summary assessment metrics (SAMs).

SAMs are averages of normalized PAMs. Here we use the empirical cumulative density function (ECDF) normalization introduced by Hoffman et al.¹⁷ as implemented by Hoffman et al.¹⁸ By normalizing PAMs, they become comparable. Using ECDF gives a theoretical basis for statistical hypothesis testing since under the null hypothesis that there is no impact, each normalized PAM has a uniform random distribution with mean 1/2 and variance 1/12. The use of SAMs increases statistical significance and avoids the problems of focusing on one particular PAM. This can be a significant challenge to traditional calibration because it is possible to improve the calibration with respect to one PAM while simultaneously reducing the degree of agreement for other PAMs.

4 MicroMAS-2 Analysis and Forecast Impact

To summarize the results of the OSSEs, selected assessments from those described in Sec. 3.2 are presented.

4.1 Analysis

In order to investigate the impact of the assimilation of MicroMAS-2 observations on the GDAS analysis, geophysical fields of the analyses from Control, Control + MicroMAS-2, 2Polar, and 2Polar + MicroMAS-2 experiments are compared to the corresponding G5NR fields for verification. The nature of an impact is determined by whether the Control + MicroMAS-2 and 2Polar + MicroMAS-2 analyses are closer to G5NR (i.e., the truth) compared to the Control and 2Polar analyses, respectively. The main impacts are expected to occur for temperature and water vapor since the MicroMAS-2 channels are directly sensitive to the profiles of temperature and water vapor. The difference of the mean absolute values of the 250 hPa temperature and 850 hPa RH analysis errors in Fig. 5 shows mostly positive impact in the tropics for both temperature and RH and for both Control + MicroMAS-2 and 2Polar + MicroMAS-2 but with higher impact for 2Polar + MicroMAS-2. We might expect higher impact in the data starved 2Polar case in general, but in addition, in the current Control experiments, MicroMAS-2 observations have less opportunity to provide new information as they are collocated with the ATMS observations. The substantial negative analysis impact seen in this figure at high southern latitudes for geopotential height, temperature, and RH is mostly restricted to areas over the Southern Ocean where sea ice is present in the austral winter. We have not identified the exact reason for this, but it may be due

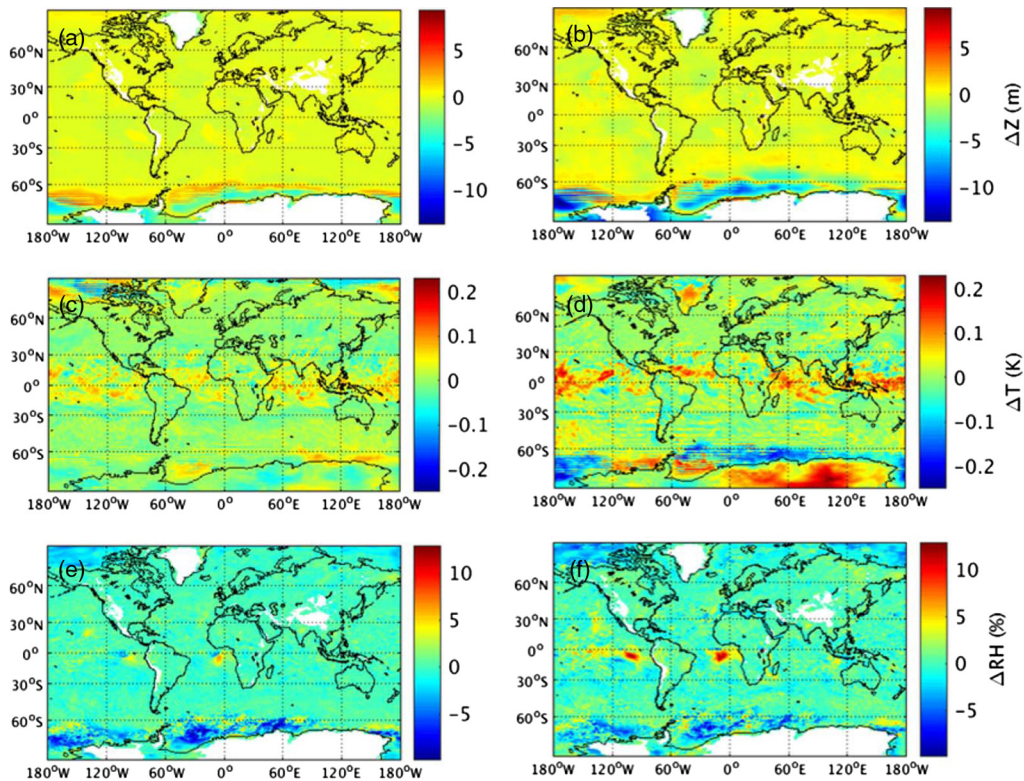


Fig. 5 The difference of the time average of the absolute values of analysis error with respect to (a, c, e) the NR for Control minus Control + MicroMAS-2 and for (b, d, f) 2Polar minus 2Polar + MicroMAS-2; (a, b) for 850 hPa geopotential height, (c, d) for 250 hPa temperature, and (e, f) for 850 hPa RH. The time average is over all analysis cycles from August 15 to September 15, 2006. Positive values indicate that MicroMAS-2 has reduced the magnitude of the analysis error.

to an inconsistency in the QC procedures or of the surface emissivity used in the two radiance calculations used in these experiments: one in simulating observations from the G5NR and the other in the observation operator of the GSI.

Table 3 summarizes the RMSE statistics for four variables (geopotential height, temperature, vector wind, and RH) and four pressure levels (250, 500, 850, and 1000 hPa). The table shows neutral or slightly positive impacts for most levels for temperature and RH, and mixed impacts for vector wind and geopotential height. The largest negative impact in the table is for 850 hPa geopotential height in the 2Polar experiments, which is consistent with the order 10 m degradation seen in Fig. 5(b) in the Southern Ocean.

4.2 Forecast

To assess the forecast impact of the assimilation of MicroMAS-2 observations, GFS forecasts from the Control, Control + MicroMAS-2, 2Polar, and 2Polar + MicroMAS-2 experiments were verified at their valid times against corresponding G5NR analyses. The general positive impact of MicroMAS-2 on global NWP forecasts is seen in the scorecards like that presented in Fig. 6. Figure 6 scorecard compares 2Polar and 2Polar + MicroMAS-2 for forecast days 1, 3, 5, and 6 (or forecast hours 24, 72, 120, and 144, respectively), initialized each day at 0000 UTC from August 15 to September 15, 2006. The metrics include AC and RMSE for different variables—geopotential height, vector wind, and temperature—at different vertical levels, over different regions—North America, NHX, SHX, and tropics. Colors and shapes reflect the improvement or degradation of the impact of adding MicroMAS-2 observations to the 2Polar constellation. Mostly positive impacts can be seen at lower pressures for geopotential height and temperature, and mostly neutral impact for vector wind at all levels. The scorecard assessing the impact of

Table 3 The global mean RMSE values of Control and Control + MicroMAS-2, 2Polar, and 2Polar + MicroMAS-2 analyses for geopotential height (m), temperature (K), vector wind (m/s), and RH (%), at 250, 500, 850, and 1000 hPa levels, verified against NR for every 6 h and averaged over August 15 to September 15, 2006. The changes are computed with respect to Control and 2Polar. A negative value in bold (lower RMSE) indicates MicroMAS-2 assimilation improves the analysis and a positive value in italic (higher RMSE) indicates MicroMAS-2 assimilation degrades the analysis.

Variable	Level	Control	Control + MicroMAS-2	Change (%)	2Polar	2Polar + MicroMAS-2	Change (%)
Geopotential height (m)	250	7.83	7.60	-2.94	8.45	8.30	-1.78
	500	6.87	7.01	+2.04	8.43	8.37	-0.71
	850	5.19	5.37	+3.47	5.76	6.26	+8.68
	1000	4.13	4.20	+1.69	4.56	4.67	+2.41
Temperature (K)	250	0.41	0.42	+0.45	0.43	0.43	-1.03
	500	0.68	0.67	-0.85	0.74	0.75	+1.90
	850	1.12	1.17	+4.06	1.28	1.28	-0.17
	1000	1.20	1.19	-0.71	1.27	1.24	-2.67
Vector wind (m/s)	250	1.83	1.83	0.00	2.10	2.10	0.00
	500	1.80	1.80	0.00	1.98	1.97	-0.51
	850	1.76	1.78	+1.14	1.95	1.96	+0.51
	1000	1.26	1.27	0.79	1.46	1.47	+0.68
RH (%)	250	13.51	13.38	-0.96	15.26	14.56	-4.59
	500	12.44	12.37	-0.56	13.78	13.35	-3.12
	850	13.40	13.59	+1.42	14.56	14.44	-0.82
	1000	7.99	7.95	-0.50	7.94	8.00	+0.76

MicroMAS-2 on the Control experiment (not shown) is similar and supports the same general conclusions.

Figures 7 and 8 show SAMs for the four experiments globally [Fig. 7(a)] and for various categories. Under the null hypothesis that there is no difference between the experiments, each SAM would have an expected value of 1/2, which is the base of the color bars, and 95% of the SAMs would be within the gray shading around 1/2. These SAMs are calculated for the categories given along the x -axes in Figs. 7(b) and 8, i.e., for eight forecast times (from 0 to 7 days), for five levels (200, 500, 700, 850, and 1000 hPa), for three domains (NHX, SHX, tropics), for four variables (Z , T , V , RH), for three statistics (AC, RMSE, bias, or AME), and for the 32 forecast verification times (August 15 to September 15, 2006).

SAMs depend on the reference sample used to determine the ECDF. To make the results of this study comparable to the results of the study of Boukabara et al.,⁷ we use the same categories and the same reference sample used in that study. In that study, the reference sample comprised experiments Control, 2Polar, and 3Polar (an experiment intermediate between Control and 2Polar), all verified versus the G5NR. The effect of the reference sample as shown in Fig. 7 (color bars versus black outlines) is to increase all SAMs by a small amount because the MicroMAS-2 experiments are generally more skillful, but the comparisons of SAMs between different experiments are generally very similar.

MicroMAS-2 makes a positive difference for the global SAMs for both Control and 2Polar configurations, and this result is nearly statistically significant for Control + MicroMAS-2 [Fig. 7(a)]. Since we are examining impacts due to additional data sources, the impacts are

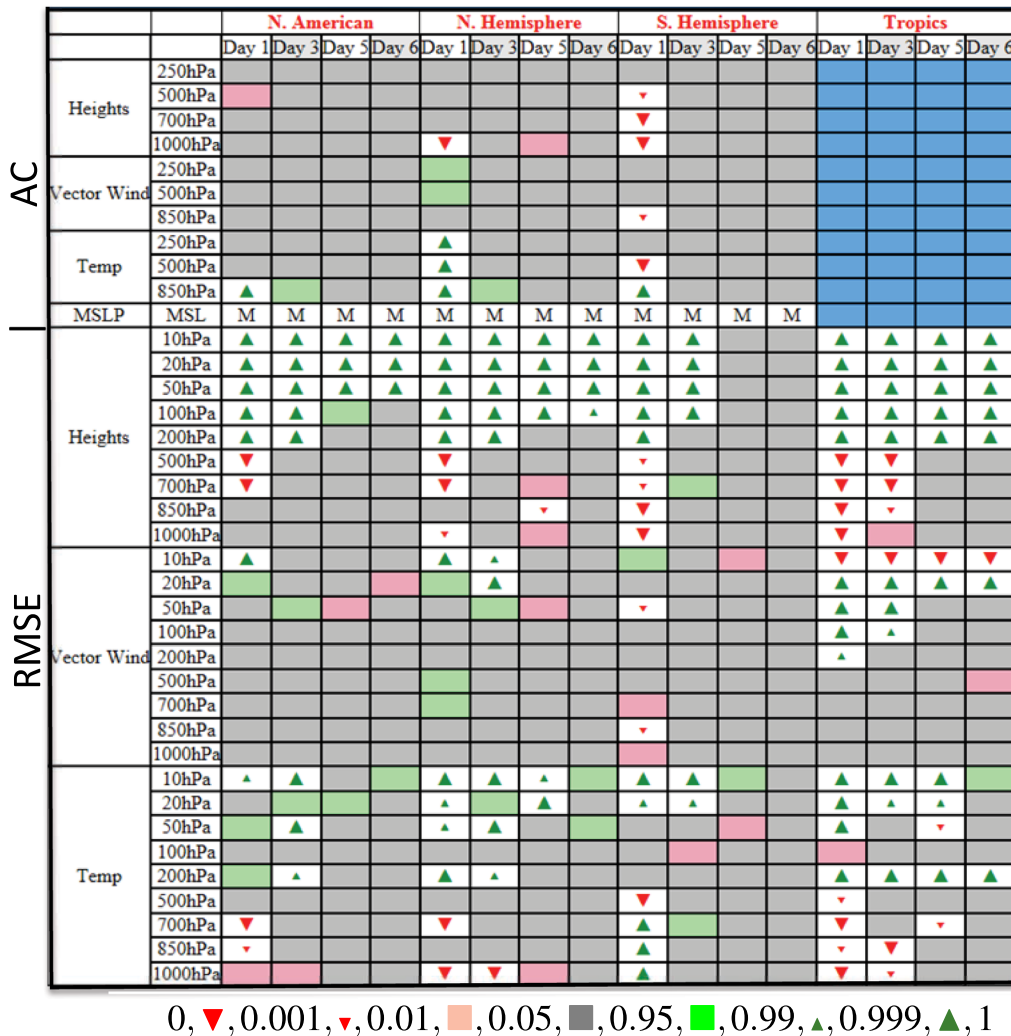


Fig. 6 Verification Statistics Data Base Scorecard for 2Polar versus 2Polar + MicroMAS-2 for forecasts validated every 0000 UTC against NR for geopotential height (heights), vector wind, and temperature (temp), for the period August 15 to September 15, 2006. The symbols and colors indicate the probability that 2Polar + MicroMAS-2 is better than 2Polar. As shown below the scorecard, the green symbols indicate that 2Polar + MicroMAS-2 is better at the 95%, 99%, and 99.9% significance levels, respectively, while the red symbols indicate that 2Polar + MicroMAS-2 is worse at the 99.9%, 99%, and 95% significance levels, respectively. Gray indicates no statistically significant differences and blue indicates that the anomaly correlations in the tropics are not considered.

expected to be largest at the start of the forecast. Indeed, at the initial time there are clear improvements, and these improvements persist to 168 h for Control + MicroMAS-2 but only to 24 h for 2Polar + MicroMAS [Fig. 7(b)]. The MicroMAS-2 experiments are significantly better for both analyses and forecasts at 250 hPa [Fig. 8(a)]. 2Polar + MicroMAS-2 is significantly better in the SHX [Fig. 8(b)]. The MicroMAS-2 experiments show improvement for all variables except for Z, and the 2Polar + MicroMAS-2 RH analysis is significantly improved [Fig. 8(c)]. The 2Polar + MicroMAS-2 analyses have significantly smaller biases than 2Polar [Fig. 8(d)]. Other differences are small and/or mixed in sign.

5 Summary and Conclusions

This study assesses the potential global NWP impact of the 12-channel passive microwave radiometer MicroMAS-2. MicroMAS-2 embodies the amazing concept of a fully functioning MW

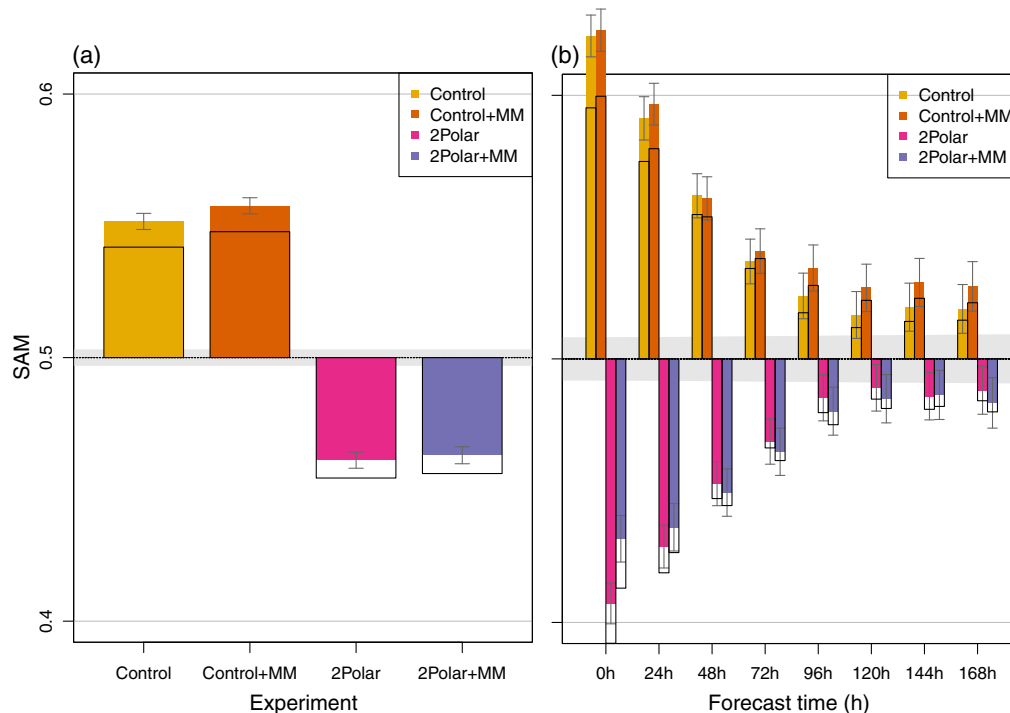


Fig. 7 Forecast impacts in terms of (a) global ECDF SAMs and (b) ECDF SAMs as a function of forecast time for each experiment (colors). Note that in these plots of SAM, confidence intervals are plotted at the 95% level and gray shading indicates the 95% null hypothesis (H_0) confidence interval. The color bars use the OSSE-OSE intercomparison reference sample of Boukabara et al.³ for ECDF normalization and the black outlines use the experiments of this study as the reference sample.¹³ Note that the forecast time zero is the SAM for the analysis error since verification is versus the G5NR.

remote sensing satellite in a 3U CubeSat—a package that could easily fit in your carry on. Details on the MicroMAS-2 project are given in Ref. 19. The assessment of the geophysical capabilities of MicroMAS-2 show that the information content is similar to operational MW sensors such as AMSU and ATMS and that the data quality from the DA point of view is in fact similar.

OSSEs conducted quantitatively estimate the expected impact of adding the MicroMAS-2 to the current global operational analysis and forecast systems or to a data gap scenario. The assimilation of the MicroMAS-2 observations into the GDAS in addition to the current operational observation system and in addition to a data gap scenario shows improvement on both analysis and forecast performance skills. MicroMAS-2 makes a positive difference for the global SAMs for both Control and 2Polar configurations, and this result is statistically significant at 250 hPa. Analyses of geopotential height are degraded, but the 2Polar + MicroMAS-2 analyses are significantly improved for RH and bias. Improvements due to MicroMAS-2 at the initial time persist to 168 h for Control + MicroMAS-2 and to 24 h for 2Polar + MicroMAS-2.

Since MW satellite observations are known to be one of the most useful of all data sources for NWP, it is perhaps not surprising that the addition of MicroMAS-2 data improves the analyses and forecasts. However, the fact that we find some significant improvements using an experimental setup that is only 1 month long is impressive in light of the following: due to the high skill of existing DA and forecast systems and the redundancy of data sources available for DA, it is very difficult to actually demonstrate positive impacts in general. In fact, it is now commonplace to run impact studies for 3 to 6 months before a new operational upgrade is approved. Further, note that Control + MicroMAS-2 assimilates both ATMS and MicroMAS-2 in the same SNPP orbit, and the impact of MicroMAS-2 would likely be greater if it were in orbit with an equatorial crossing time different than other MW sensors in the current system. Also, the weights used in the assimilation have not been optimized for MicroMAS-2.

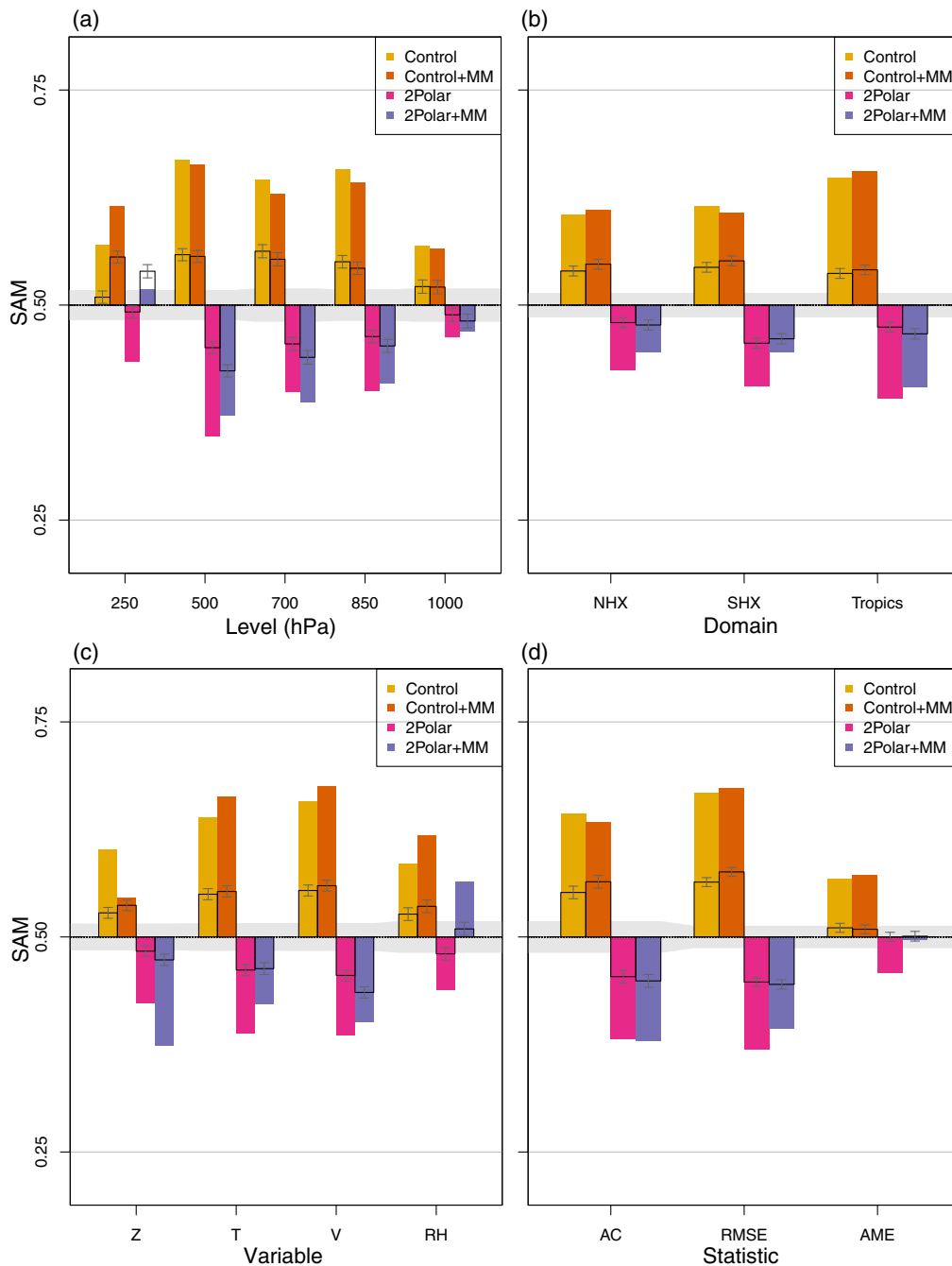


Fig. 8 Forecast impacts in terms of analysis (color bars) and forecast (black outlines) ECDF SAMs by (a) level (hPa), (b) domain, (c) variable, and (d) statistic for each experiment (colors). In this figure, confidence intervals are plotted at the 95% level for the forecast SAMs (forecast hours 24 to 168) and gray shading indicates the 95% null hypothesis (H0) confidence interval for the analysis SAMs (forecast hour 0 only).

Using observations with no explicitly added errors is a limitation of the experiments described here. Clearly, such an experiment cannot examine the impact of different observation error. However, such experiments are adequate to examine how analysis and forecast impacts qualitatively vary with observation types (temperature versus wind), spatial and temporal observing patterns (polar versus equatorial orbit), and observation vertical resolution (i.e., different channel characteristics that influence the sensor weighting functions). Furthermore, as shown by Boukabara et al.,⁷ quantitative relative impacts (as measured by SAMs for example) from “perfect” observation OSSEs are a very close match to similar impacts in real data OSEs.

Although no explicit observation errors were added in any of the OSSEs, the effect of normalization of the PAMs results in close agreement of the SAMs. Of course, the PAMs predicted by the error-free OSSEs will be too optimistic, but the SAMs are reliable for use in further analysis. As a consequence, the SAM results of the experiments reported here are directly applicable since these SAMs are calculated exactly as was done by Boukabara et al.⁷

An extension to the current study would be to conduct OSEs using the actual MicroMAS-2 observations. A follow-on to the MicroMAS-2 project is the Earth Observing Nanosatellite–Microwave (EON-MW) sensor. Our team has conducted a thorough geophysical capability assessment and a series of OSSEs for EON-MW that will be reported shortly. To mitigate some of the risks identified in the MicroMAS-2 project, the EON-MW channel set and observation characteristics are very close to those of ATMS. Due to its low costs, EON-MW might be launched in multiples, as in the proposed NASA mission “Time-Resolved Observations of Precipitation structure and storm Intensity with a Constellation of Smallsats” or TROPICS, and in the NOAA EON-MW CubeSat mission.²⁰ With multiple SmallSats carrying MW sensors, it will be possible to gather more detailed, more frequent images of severe weather, and tropical cyclones to improve modeling and forecasting of severe weather and tropical cyclone impacts.

Acknowledgments

The authors thank the many colleagues and collaborating scientists who contributed to this study: R. Atlas has been the authors’ leading mentor for OSSE research. Scientific contributions were made by E. Maddy (RTi), S. Casey (AOML/CIMAS), and K. Kumar (RTi). Many scientists developed the CRTM and CGOP, including scientists at NOAA NESDIS STAR, AOML/CIMAS, and CIMSS/SSEC, and at other institutions, including in particular at NASA GMAO where the G5N was produced. MIT/LL shared details of their design of MicroMAS-2. Grateful acknowledgement is made to the funding provided by NOAA and particularly by the NOAA National Environmental Satellite, Data, and Information Service (NESDIS) Office of Projects, Planning, and Analysis (OPPA) and by several NOAA grants. This study was partially supported by NOAA Grant NA14NES4320003 (Cooperative Institute for Climate and Satellites, CICS) at the University of Maryland/ESSIC.

References

1. W. J. Blackwell et al., “An overview of the TROPICS NASA earth venture mission,” *Q. J. R. Meteorolog. Soc.* **144**, 16–26 (2018).
2. R. Atlas et al., “Simulation studies of the impact of future observing systems on weather prediction,” in *Seventh Conf. Numer. Weather Predict.*, American Meteorological Society, Montreal, QC, Canada, pp. 145–151 (1985).
3. R. N. Hoffman and R. Atlas, “Future observing system simulation experiments,” *Bull. Am. Meteorol. Soc.* **97**, 1601–1616 (2016).
4. Z. Li et al., “The alternative of CubeSat-based advanced infrared and microwave sounders for high impact weather forecasting,” *Atmos. Oceanic Sci. Lett.* **12**(2), 80–90 (2019).
5. S.-A. Boukabara et al., “Community global observing system simulation experiment (OSSE) package (CGOP): description and usage,” *J. Atmos. Oceanic Technol.* **33**, 1759–1777 (2016).
6. S.-A. Boukabara et al., “Community global observing system simulation experiment (OSSE) package (CGOP): perfect observations simulation validation,” *J. Atmos. Oceanic Technol.* **35**, 207–226 (2018).
7. S.-A. Boukabara et al., “Community global observing system simulation experiment (OSSE) package (CGOP): assessment and validation of the OSSE system using an OSSE-OSE intercomparison of summary assessment metrics,” *J. Atmos. Oceanic Technol.* **35**, 2061–2078 (2018).
8. W. M. Putman et al., “A 7-km non-hydrostatic global mesoscale simulation for OSSEs with the Goddard Earth Observing System model (GEOS-5),” in *19th Conf. Integr. Obs.*

- and Assimilation Syst. Atmos., Oceans, and Land Surf. (IOAS-AOLS), American Meteorological Society, Boston, Massachusetts, (Phoenix, Arizona), Paper 3.1 (2015).
9. Y. Chen, Y. Han, and F. Weng, "Comparison of two transmittance algorithms in the community radiative transfer model: application to AVHRR," *J. Geophys. Res.* **117**, D06206 (2012).
 10. T. Zhu et al., "Synthetic radiance simulation and evaluation for a joint observing system simulation experiment," *J. Geophys. Res. Atmos.* **117**, D23111 (2012).
 11. L. Cucurull, J. C. Derber, and R. J. Purser, "A bending angle forward operator for global positioning system radio occultation measurements," *J. Geophys. Res. Atmos.* **118**, 14–28 (2013).
 12. R. M. Errico et al., "Development and validation of observing-system simulation experiments at NASA's Global Modeling and Assimilation Office," *Q. J. R. Meteorolog. Soc.* **139**, 1162–1178 (2013).
 13. D. T. Kleist and K. Ide, "An OSSE-based evaluation of hybrid variational-ensemble data assimilation for the NCEP GFS. Part I: system description and 3D-hybrid results," *Mon. Weather Rev.* **143**, 433–451 (2015).
 14. D. T. Kleist and K. Ide, "An OSSE-based evaluation of hybrid variational-ensemble data assimilation for the NCEP GFS. Part II: 4DVar and hybrid variants," *Mon. Weather Rev.* **143**, 452–470 (2015).
 15. S. A. Clough et al., "Atmospheric radiative transfer modeling: a summary of the AER codes," *J. Quant. Spectrosc. Radiat. Transfer* **91**, 233–244 (2005).
 16. W. J. Blackwell, "New small satellite capabilities for microwave atmospheric remote sensing," in *21st Conf. Integr. Obs. and Assimilation Syst. Atmos., Oceans, and Land Surf. (IOAS-AOLS)*, American Meteorological Society, Boston, Massachusetts, (Seattle, Washington), Paper J11.2 (2017).
 17. R. N. Hoffman et al., "An empirical cumulative density function approach to defining summary NWP forecast assessment metrics," *Mon. Weather Rev.* **145**, 1427–1435 (2017).
 18. R. N. Hoffman et al., "Progress in forecast skill at three leading global operational NWP centers during 2015–2017 as seen in summary assessment metrics (SAMs)," *Weather Forecasting* **33**, 1661–1679 (2018).
 19. H. J. Kramer et al., "Observation of the earth and its environment: survey of missions and sensors," <https://directory.eoportal.org/web/eoportal/satellite-missions/content/-/article/micromas-2>
 20. W. J. Blackwell and S. Braun, "Time-resolved observations precipitation structure and storm intensity with a constellation of smallsats," <https://tropics.ll.mit.edu/CMS/tropics/>.

Narges Shahroudi is an expert in satellite remote sensing, impact studies of satellite observations, and applications of machine learning techniques for satellite data processing and weather forecasting. She is an analyst at NOAA/NESDIS Center for Satellite Applications and Research (STAR) and is employed by Riverside Technology Inc.

Yan Zhou is expert in data assimilation (DA), numerical weather prediction (NWP), big data analytics, and satellite remote sensing. She is a research scientist at NOAA/NESDIS Center for Satellite Applications and Research (STAR) and is employed by University of Maryland Earth System Science Interdisciplinary Center (ESSIC).

Sid-Ahmed Boukabara is an expert in remote sensing and NWP satellite data assimilation of the earth's atmosphere and surface from space-borne infrared and microwave sensors. He is a principal scientist at the NOAA/NESDIS Center for Satellite Applications and Research (STAR). His interests include (1) variational algorithms and data assimilation approaches, (2) observing systems impact assessments, and (3) environment data fusion. Currently, he is engaged in strategic new initiatives and pilot projects to explore innovative technologies and numerical approaches.

Kayo Ide is an associate professor at the University of Maryland and in the Earth System Science Interdisciplinary Center. With background in engineering, theoretical fluid dynamics

and applied mathematics, she studies Earth system sciences from interdisciplinary perspectives. Her primary research interests are scientific prediction for earth systems and mixing and transport in geophysical fluids.

Tong Zhu is an expert in radiative transfer modeling and the impact of satellite observations on NWP. He is one of the CRTM core developers. He is a research scientist at the Cooperative Institute for Research in the Atmosphere and is employed by Colorado State University.

Ross Hoffman is the past vice president of the R & D division of Atmospheric Environmental Research (AER 1999 to 2013). He is now a part-time scientist at NOAA/NESDIS STAR/ University of Maryland (CICS). His principal areas of interest are objective analysis and assimilation methods, impact experiments, atmospheric dynamics, climate theory, and atmospheric radiation.